

# PHYSICAL AND TECHNOLOGICAL ASPECTS OF a-Si:H/c-Si HETERO-JUNCTION SOLAR CELLS

M. Schmidt, H. Angermann, E. Conrad, L. Korte, A. Laades, K. v. Maydell, Ch. Schubert, R. Stangl  
Hahn-Meitner-Institute Berlin (HMI), Kekuléstr. 5, D-12489 Berlin, Germany

Corresponding author: Tel: +49/30/8062-1352, Fax: +49/30/8062-1333, e-mail: [schmidt-m@hmi.de](mailto:schmidt-m@hmi.de)

## ABSTRACT

We report on the basic properties of a-Si:H/c-Si hetero-junctions, their effects on the recombination of excess carriers and its influence on the a-Si:H/c-Si hetero-junction solar cells. For this purpose we measured the gap state density distribution in thin a-Si:H layers, determined its dependence on deposition temperature and doping by an improved version of near UV-photoelectron emission spectroscopy. Furthermore, the Fermi level position in the a-Si:H and the valence band offset were directly measured. In combination with interface specific methods such as surface photovoltage analysis and our numerical simulation program AFORS-HET, we are able to find out the optimum in wafer pretreatment, doping and deposition temperature for efficient a-Si:H/c-Si solar cells without an i-type a-Si:H buffer layer. By a deposition at 210°C with an emitter doping of 2000 ppm of B<sub>2</sub>H<sub>6</sub> on a well cleaned pyramidal structured c-Si(p) wafer we reached 19.8 % certified efficiency.

## INTRODUCTION

The prior goal of photovoltaics is the cost reduction of the generated electrical energy and their world wide availability. One way to achieve this goal is the further improvement of the efficiency of the solar cells (panels) near to the thermodynamic efficiency limit. Hetero-junction solar cells represent a possible concept for reaching this limit [1].

An inherent advantage of hetero p/n-junctions is the possibility to choose materials, layer thicknesses, dopant concentrations etc. for their construction which are best suited reaching efficiencies near to the thermodynamic solar conversion limit for silicon of about 29 % [2]. The a-Si:H(n,p)/c-Si(p,n) system represents one possible example. Such cells with an extremely thin i-type a-Si:H buffer layer inserted into each hetero-junction were realized by Sanyo [3] and reach efficiencies near 21 %. The main challenge is to avoid recombination at the a-Si:H/c-Si hetero-interfaces which form both the emitter/substrate- and the substrate/rear-contact. The key quantities of a hetero-junction, shown in Fig. 1, are the electronic properties of the a-Si:H layer, the a-Si:H/c-Si band-offsets  $\Delta E_V$ ,  $\Delta E_C$ , the hetero-interface state density distribution  $D_{it}(E)$ , the band bending  $q\phi_{SO}$  and the minority diffusion length in the c-Si substrate  $L_D$ . We developed appropriate analytical and numerical techniques like near-UV-photoelectron spectroscopy

NUV-PES for analyzing the electronic properties of thin a-Si:H layers [4] and improved the surface photovoltage method in order to detect the interface state density, interface recombination and band bending in the a-Si:H/c-Si hetero-structure. We determined the key parameters and analyzed their influence on solar cell characteristics using standard solar cell measurements and the AFORS-HET simulation program which is a proprietary development free for public use [5].

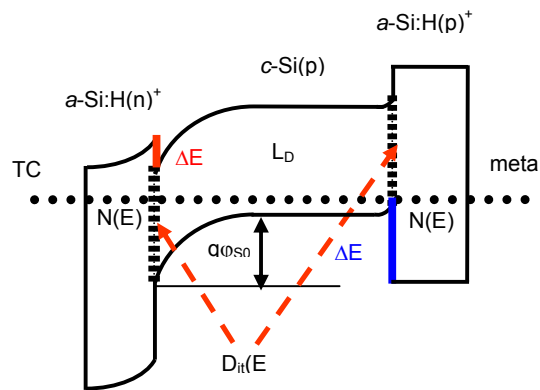


Fig. 1. Band scheme of the a-Si:H/c-Si hetero-junction embedded into a complete TCO/a-Si:H(n<sup>+</sup>)/c-Si(p)/a-Si:H(p<sup>+</sup>) solar cell structure. The terms are explained in the text.

Since the quality of the hetero-junctions is determined by the first mono-layers of the hetero-transition adequate techniques are necessary which allow the preparation of the hetero-interface and its characterization on an atomic depth scale.

## SILICON SURFACE PRETREATMENT

The a-Si:H emitter deposition requires c-Si substrates with undamaged, contamination-free and chemically stable silicon surfaces because the silicon surface becomes part of the hetero-interface which "remembers" the initial silicon surface state. Many applications additionally necessitate special crystallographic configurations of the silicon substrate surface: silicon wafers with randomly distributed upside pyramids, textured by anisotropic etching are used to optimize the light trapping properties.

Non-destructive and surface sensitive techniques such as the large-signal field-modulated surface photovoltage (SPV) method [6] and spectroscopic ellipsometry (SE) [7] have been utilized to investigate the relation between structural imperfections at silicon surfaces, interface state densities and stability of surface passivation. Both, the density of surface states on H-terminated surfaces and the resistance against native oxidation in clean-room air were found to be strongly related to the interface micro-roughness [8].

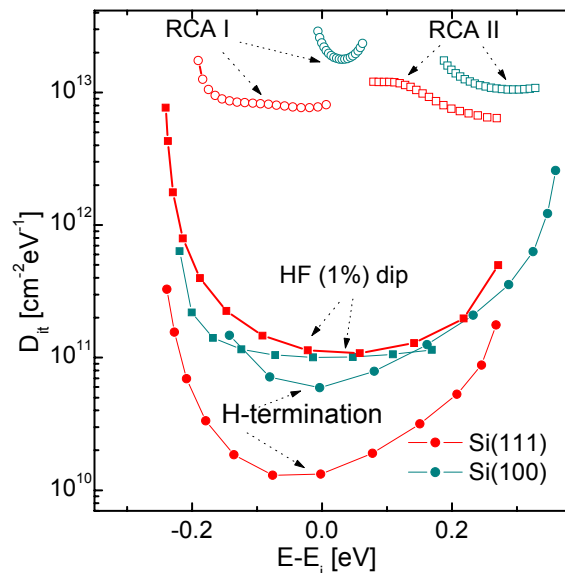


Fig. 2. Energetic distributions of surface states  $D_{it}(E)$  obtained on Si(111) and Si(100) surfaces after RCA-I, RCA-II, HF-dip and H-termination. The H-termination was carried out by a sequence of hot water oxidation and removing the oxide layers in  $\text{NH}_4\text{F}$  solution [8]. The resulting H-terminated surface state distributions were measured immediately after  $\text{NH}_4\text{F}$ -etching.

After RCA cleaning, a high density of surface states  $D_{it}(E)$  was observed. Conventional HF treatment (HF-dip) reduces the surface state density. The Density of rechargeable surface states can be further reduced by preparing atomically flat silicon surfaces and well-ordered silicon surfaces through the application of special hot water oxidation and H-termination procedures. It was shown that the ideally H-terminated surface is characterized by a very low density of surface states [8]. It is comparable to well thermally oxidized surfaces.

The densities of interface states on the initially H-terminated silicon surfaces were found to increase drastically during the first monolayer of oxide growth. The duration of the initial phase of oxidation in air ranges from a couple of minutes on HF-treated surfaces up to some hours on conventionally H-terminated surfaces and Si(100) substrates. Highest stabilities in clean-room air with initial phases up to 48 h have been found on Si(111) by applying a special H-termination procedure. Further on, it was shown that by storage in dry nitrogen atmosphere,

the re-oxidation of H-terminated surfaces can be decelerated, but not completely prevented, because of reactions with moisture adsorbates. Consequently, the time between surface cleaning, smoothing, H-passivation and the a-Si:H deposition has to be as short as possible.

## DEPOSITION OF a-Si:H

Flat Si surfaces or KOH/IPA pyramid etched surfaces followed by a HF-dip and/or H-termination were used as substrates, depending on the experimental task. The a-Si:H was deposited by conventional 13.56 MHz plasma enhanced chemical vapor deposition on float zone grown single crystalline silicon wafers ( $1-2 \Omega\text{cm}$ ). Doping of a-Si:H was achieved by mixing  $\text{SiH}_4$  with  $\text{H}_2$ -diluted  $\text{PH}_3$  and  $\text{H}_2$ -diluted  $\text{B}_2\text{H}_6$  for n-type and p-type doping, respectively. The deposition temperature in both cases was adjustable between  $60^\circ\text{C}$  and  $300^\circ\text{C}$ . The optimized value amounts to about  $210^\circ\text{C}$ . In the case of solar cell preparation the transparent conducting oxide ZnO:Al was sputtered on top of the a-Si:H emitter to improve the surface conductance. On the rear side of the structure an a-Si:H layer with the same conductivity type as the c-Si wafer was deposited. Aluminum was used for the rear contact. Solar cell devices were prepared by photolithographic lift-off for the front grid and the emitter area ( $1 \text{ cm}^2$ ) was defined by MESA-etching.

## ELECTRONIC PROPERTIES OF THIN a-Si:H

The a-Si:H layer thickness  $d$  shows an optimum for application as emitter at about  $5 \text{ nm} < d \leq 10 \text{ nm}$ . This follows from the experimental results of solar cell data in [3,9] and our numerical simulations of the open circuit voltage  $V_{oc}(d)$  and the short circuit values  $I_{sc}(d)$ . Such layer thicknesses correspond to a sequence of about 20-40 Si-H bonding length. For such extremely thin layers we have to determine the Fermi level position, the gap state density distribution  $N(E)$  and the band offsets with the adjacent crystalline silicon.

An adequate method for measuring the electronic structure of the 5-10 nm thin a-Si:H emitter is photoelectron emission spectroscopy excited by near-ultra-violet light, NUV-PES [4,10,11,12]. The NUV-excitation leads to an increased electron escape depth of up to 10 nm. This is attributed to the absence of surface or bulk plasmon generation which need energies of about 10 eV well above the UV excitation energies of  $h\nu = 3-8 \text{ eV}$ . Furthermore, the optical excitation probability in this energy region increases by several orders of magnitude compared to excitation with soft X-rays. Photoelectron spectroscopy measurements of the internal yield  $Y_{int}$  of the emitted photoelectrons were carried out in constant final state yield spectroscopy mode, CFSYS, by varying the photon energy,  $h\nu = 3-8 \text{ eV}$  at fixed energy analyzer detection energy [4,11].

From  $Y_{int}(E_{kin}, h\nu) \propto N_{occ}(E_{kin} - h\nu)$  we obtain the absolute values of the density of occupied states  $N_{occ}(E)$  by normalization of  $Y_{int}$  at the valence band edge,  $E_V$ , to  $2 \times 10^{21} \text{ cm}^{-3} \text{ eV}^{-1}$  [12].  $E_V$  is determined from a fit of a model DOS, broadened by the experimental resolution to

the measured spectrum. Due to the limited photon penetration and electron escape depth, the measured distribution is a weighted average of the DOS of the sample up to a depth of 7-10 nm. The direct observation of the density distribution  $N_{\text{occ}}(E)$  of occupied gap states down to  $10^{14} \text{ cm}^{-3} \text{ eV}^{-1}$  is possible, details can be found in [11]. In addition, the Fermi level position can be determined with an energy resolution of  $\sim 100 \text{ meV}$ . Fig. 3 shows that the Fermi level shifts from 0.45 eV below the conduction band via 0.2 eV above the intrinsic level to 0.41 eV above the valence band edge for  $\text{PH}_3$ -doped, intentionally undoped and  $\text{B}_2\text{H}_6$  a-Si:H layers, respectively.

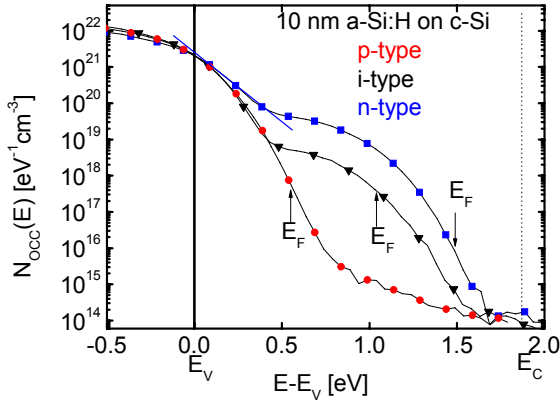


Fig. 3. Density of occupied gap states  $N_{\text{occ}}(E)$ , measured by constant final state yield spectroscopy, of a series of a-Si:H layers deposited by PECVD at  $210^\circ\text{C}$  on c-Si(p). The a-Si:H doping (gas phase concentration) amounts to  $10^4$  ppm  $\text{B}_2\text{H}_6:\text{SiH}_4$  (p-type),  $10^4$  ppm  $\text{PH}_3:\text{SiH}_4$  (n-type), without doping (i-type). The valence band edge  $E_V$  is chosen as origin of the abscissa. Arrows mark the Fermi level positions.

$N_{\text{occ}}(E)$  of the n-type sample in Fig. 3 clearly indicates the band tail states near the valence band edge, characterized by the slope of the straight line, the so called Urbach energy, and the Gaussian distributed deep dangling bond defects  $N_D$ , located about 0.65 eV above the valence band edge.

For extremely thin a-Si:H(n) layers on c-Si, we obtain a contribution of c-Si valence band states to the photoemission signal. The deviation of the  $N_{\text{occ}}(E)$ -slope for the 2.8 nm thin a-Si:H layer shown in Fig. 4 sets in at  $E-E_V \sim 0.45 \text{ eV}$ . This allows the exact determination of the band offset between a-Si:H(n) and c-Si(p,<111>). This was cross-checked for a-Si:H(p) on c-Si(n,<111>), which gave in both cases values of  $\Delta E_V = 0.46 \pm 0.05 \text{ eV}$  and  $\Delta E_C = 0.14 \pm 0.10 \text{ eV}$ . The latter value follows from the a-Si:H band gap of  $1.72 \pm 0.05 \text{ eV}$ , which was measured by spectral dependent photoconductivity of 50 nm thick a-Si:H layers.

The knowledge of reliable bandoffset values is very important for the application of a-Si:H/c-Si hetero-structures in devices such as solar cells, because charge transfer and recombination activity depend on the band offset and the Fermi level position at the interface. Fig. 5 illustrates the influence of both the band offset for

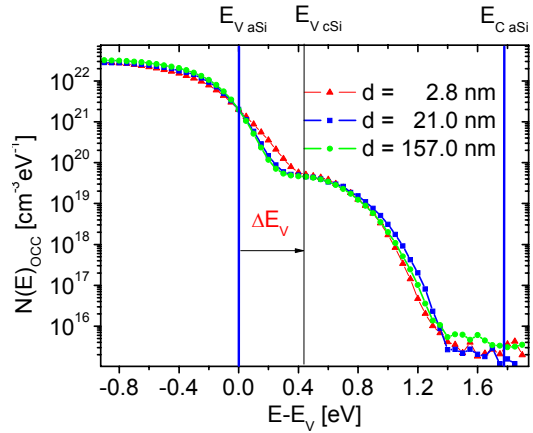


Fig. 4.  $N_{\text{occ}}(E)$  of a nominally undoped a-Si:H thickness series on c-Si(p) prepared at  $170^\circ\text{C}$  by PECVD. The CFSYS-spectra were excited with  $h\nu = 5.0\text{-}7.8 \text{ eV}$ .

minority charge carriers and of the interface state density at the a-Si:H/c-Si interface on the solar cell efficiencies of the a-Si:H(n)/c-Si(p)-type. The calculations were realized using our AFORS-HET program [5].

From Fig. 5 and the corresponding calculations in [9] it becomes clear that the a-Si:H(p)/c-Si(n)-type heterojunction with a minority carrier band offset of  $\Delta E_V = 0.46 \text{ eV}$  is less sensitive against interface recombination. This emphasizes that recombination at the amorphous/crystalline silicon interface is one key parameter, that can reduce the solar cell performance of TCO/a-Si:H/c-Si solar cells significantly.

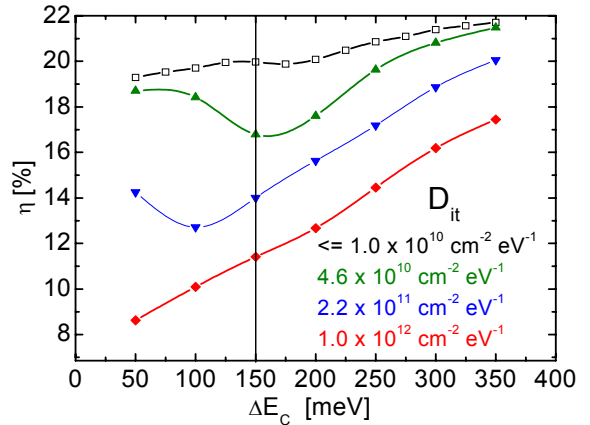


Fig. 5. Calculated dependence of a-Si:H(n)/c-Si(p) solar cell efficiency on the minority charge carrier band offset with a variation of interface state density  $D_{\text{it}}(E)$  as parameter. The rear side recombination velocity was set to  $10^7 \text{ cm}\cdot\text{s}^{-1}$  and  $L_D = 400 \mu\text{m}$ .

In order to study the band bending, interface state densities and effective interface recombination, excess carriers are optically generated in the c-Si absorber of Si/SiO<sub>2</sub> and a-Si:H/c-Si hetero-structures and the surface

photovoltage method (SPV) and photoluminescence measurements (PL) were applied.

In SPV measurements, the sample under test is sandwiched in a structure consisting of a transparent conductive front contact (TCO), an insulating slab of mica, the sample and a metallic back contact. Thus, an artificial metal-insulator-semiconductor (MIS) structure is created. Upon intense illumination of the sample by a laser pulse ( $h\nu = 1.35$  eV, pulse duration 160 ns, intensity  $10^{19}$  photons/( $\text{cm}^2$  s)) through the TCO, excess charge carriers are generated in the c-Si, leading to a flattening of the bands and a split-up of the quasi-Fermi levels of electrons and holes. The surface photovoltage of the sample is then measured capacitively via the insulating slab as photovoltage pulse  $V_{\text{SPV}}$ . The sample is illuminated at a photon energy smaller than the band gap of a-Si:H ( $\sim 1.7$  eV). Thus, the latter acts as an additional window layer, the excitation of charge carriers takes place in the crystalline substrate and their main recombination path is via the defect states at the a-Si:H/c-Si interface. From measurements of  $V_{\text{SPV}}$  depending on the external field, the distribution  $D_{\text{it}}$  of a-Si:H/c-Si interface gap states can be calculated [6]. The precondition is that no change of the charge state of the a-Si:H and of the interface states takes place during the light pulse. The results of such investigations are shown in Fig. 2 and Fig. 6.

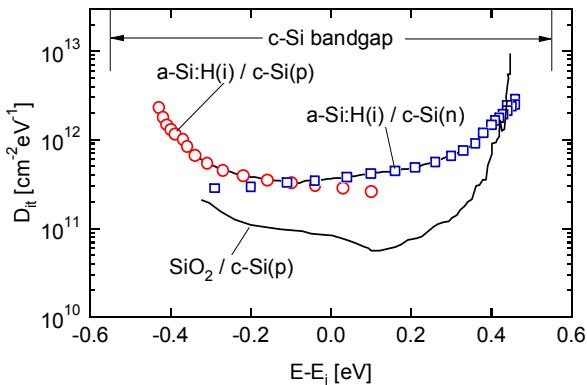


Fig. 6.  $D_{\text{it}}(E)$  vs.  $E$  for 10 nm a-Si:H(i)/c-Si(p,n, (111)) structures resulting from field dependent  $V_{\text{SPV}}$  measurements, realized at 118K. For comparison  $D_{\text{it}}(E)$  of 100 nm thermally grown oxide (1000°C) on c-Si(n, (100)) followed by forming gas annealing (450°C, 30 min) is shown, which was measured at 295 K.

A comparison of the  $D_{\text{it}}(E)$  spectra of Si/SiO<sub>2</sub> (thermally grown at 1100°C in dry O<sub>2</sub> followed by forming gas annealing) with the a-Si:H(i)/c-Si heterojunction shows a similar distribution and a low quantitative difference. The SPV measurements have been done at i-type a-Si:H because only undoped layers allow the field modulation of band bending in c-Si. Deep temperatures were needed (120 K) to suppress recharging effects of the a-Si:H during the laser pulse excitation. This effect can not be completely excluded so that the measured  $D_{\text{it}}(E)$  spectrum gives an upper limit of the true interface state

distribution, which indicates a very well passivated a-Si:H/c-Si interface. This is in good agreement with measured interface recombination velocities below  $10$   $\text{cm}\cdot\text{s}^{-1}$  [15]. On the other hand such recharging effects indicate that a-Si:H itself may contribute to the recombination via a-Si:H gap-states. This poses the question how the deposition conditions such as temperature and doping influence the a-Si:H properties and the interface recombination. To answer this question, we compared  $V_{\text{SPV}}(t)$ ,  $I_{\text{PL}}$  and  $N_{\text{OCC}}(E)$  of a-Si:H/c-Si heterostructures prepared at different deposition temperatures, as shown in Figs. 7, 8 and 9.

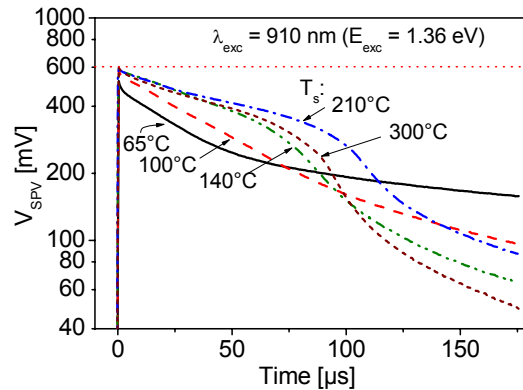


Fig. 7. Decay of  $V_{\text{SPV}}$  vs. time for 10 nm thick a-Si:H(i) on c-Si(p,(111)) prepared at different deposition temperatures. The measurements were performed at room temperature. The dotted straight line marks the maximum of detected photovoltage of 600 mV, which corresponds to the initial band bending in c-Si.

The relaxation of the SPV-signal to thermal equilibrium due to recombination of excess charge carriers is detected as a measure for interface passivation. The surface photovoltage  $V_{\text{SPV}}(\delta n)$  saturates at high excess charge carrier densities,  $\delta n$ , and depends in a strongly non-linear fashion on  $\delta n$ . This explains qualitatively the shape of  $V_{\text{SPV}}(t)$ , which starts in the high excitation (saturation) regime, characterized by a time constant  $\tau_{\text{H}}$  and drops off after certain times into the low excitation regime. For details see [13,14].  $\tau_{\text{H}}$  correlates well with the photoluminescence signal  $I_{\text{PL}}$ , because the latter one is also proportional to  $\delta n$ .

Both parameters,  $\tau_{\text{H}}$  and  $I_{\text{PL}}$ , characterize the effective recombination at the a-Si:H/c-Si interface. They are used to optimize process parameters of a-Si:H with regard to minimizing the interface recombination. From Figs. 7 and 8 it clearly results that a minimum of effective interface recombination is reached at a-Si:H deposition temperatures of about 210°C.

The Urbach energy  $E_{\text{OV}}$  and the Fermi level position  $E_{\text{F}}-E_{\text{V}}$  of a-Si:H(i) type layers show also the most ideal values for deposition temperatures around 210°C, as presented in Fig. 9. This indicates a minimum of strained bond density ( $E_{\text{OV}}$ ) and reduced Fermi level pinning at this deposition temperature. Details of the NUV-PES investigations are given in [11,16]. Besides the a-SiH

deposition temperature, the a-Si:H doping also has great impact on the interface properties.

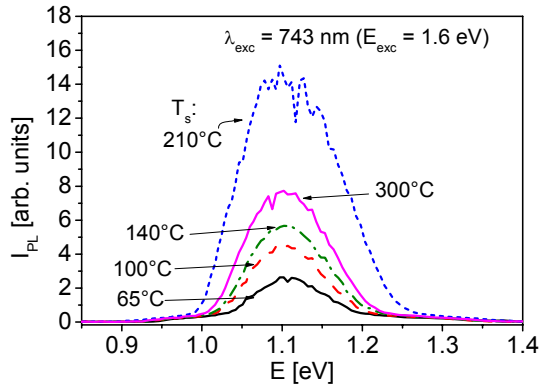


Fig. 8: PL spectra recorded from c-Si(p) substrates covered with a-Si:H(n) deposited at different substrate temperatures  $T_s$ . The measurements were performed at room temperature.

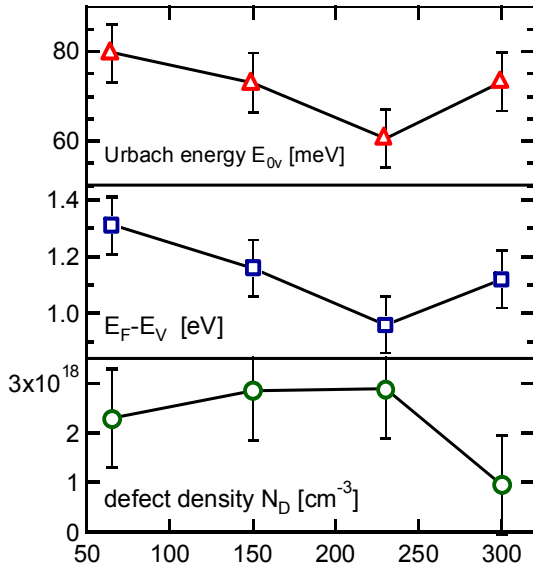


Fig. 9:  $E_{ov}$ ,  $E_F - E_V$  and  $N_D$  in dependence of deposition temperature for 10 nm thick a-Si:H(i) layers on c-Si(p) measured by CFSYS in the NUV region (4-7.5 eV).

We found the optimum of a-Si:H(n,p) emitter-doping at about 1000-2000 ppm  $\text{PH}_3$  and  $\text{B}_2\text{H}_6$  gas phase concentration [18]. From all these investigations results a connection between the Urbach energy and the effective interface recombination. To what extent this is related to the charge carrier transfer from c-Si to a-Si:H via tail states or a similar dependence of the interface state density on the deposition conditions remains an open question.

The influence of both interfaces to the hetero-junction solar cell performance was calculated, see Fig. 10. For

the front hetero-junction (a-Si:H(n)/c-Si(p)) we assumed different interface state densities and the rear side hetero-interface (a-Si:H(p<sup>+</sup>)/c-Si(p)) is characterized by two recombination velocities. These data were calculated using AFORS-HET [5].

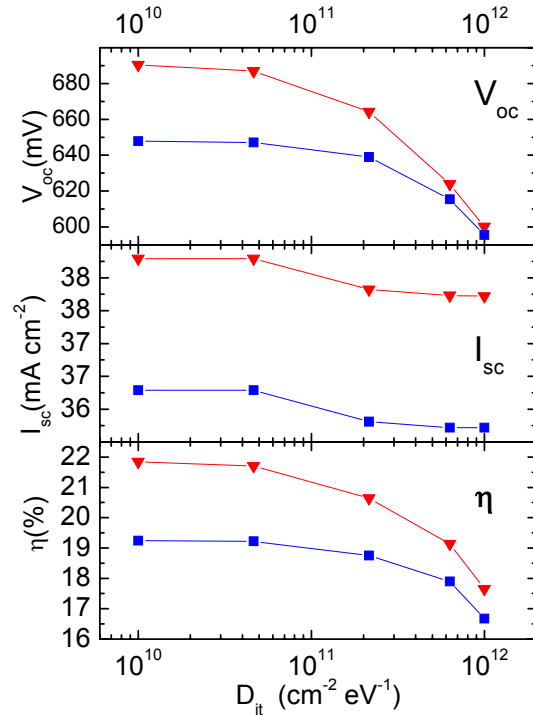


Fig. 10: Calculated  $V_{oc}$ ,  $I_{sc}$  and  $\eta$  in dependence of the front side interface state density with rear side recombination velocities of  $10^2 \text{ cm} \cdot \text{s}^{-1}$  (red curves) and  $10^6 \text{ cm} \cdot \text{s}^{-1}$  (blue curves). The calculations were performed for a TCO/a-Si:H(n)/c-Si(p)/a-Si:H(p)/Al solar cell structure with  $L_D = 400 \mu\text{m}$ ,  $d_{\text{TCO}} = 80 \text{ nm}$ ,  $d_{\text{a-SiH}(n)} = 10 \text{ nm}$ .

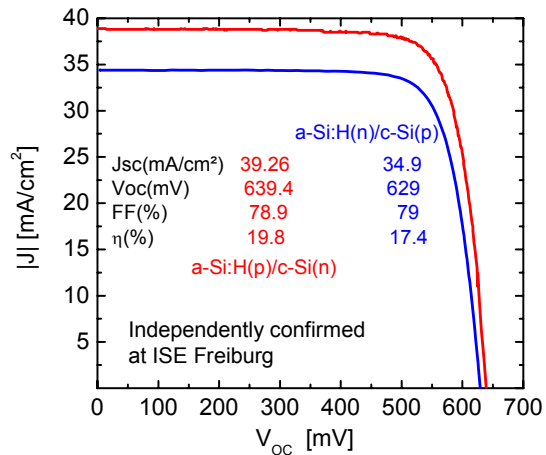


Fig. 11: Hetero-junction solar cell characteristics for both types of hetero-junction solar cells TCO/a-Si:(n)/c-Si(p)/a-Si:(p<sup>+</sup>) and a-Si:H(p)/c-Si(n)/a-Si:(n<sup>+</sup>).

It is clearly shown, that an increasing front side interface state density decreases  $V_{OC}$  by enhanced recombination, because this leads to a reduced Fermi level splitting under illumination. The rear side recombination works like a constant loss mechanism on  $I_{SC}$  and reduces  $V_{OC}$  by 40 mV at maximum. For the calculations data were utilized measured by NUV-PES and SPV measurements. The optical data of ZnO related absorption and reduced reflection by pyramidal c-Si surfaces are taken into account as well. For the inversely doped hetero solar cell structure, TCO/a-Si:H(p)/c-Si(n)/a-Si:H(n<sup>+</sup>), we obtain at maximum 25 % calculated efficiency. Applying the optimized preparation parameters with respect to recombination and cell efficiencies we reached 17.4 % of an a-Si:H(n)/c-Si(p)/a-Si:H(p) hetero-junction solar cell and 19.8 % for an a-Si:H(p)/c-Si(n)/a-Si:H(n) structure as shown in Fig.11, which were certified by ISE Freiburg.

### Conclusion

The analysis of the basic parameters has improved our physical understanding of the a-Si:H/c-Si system, which represents a model system of silicon based hetero-junctions. For applying this structure as solar cell we obtained valuable hints on the most relevant parameters. If we compare the calculated with the measured data we notice that there exists a potential for improving the solar cell efficiency further, predominantly by reducing the interface recombination [19]. Systematic analyses of plasma post-treatment and annealing processes as well as modifications of the wafer pre-cleaning procedure are under way.

### Acknowledgement

This work was financially supported by the German Bundesministerium für Bildung und Forschung: contract number 01SF0012. The authors would like to thank K. Jacob, C. Klimm and D. Patzek for technical support.

### References

- [1] R. M. Swanson, „Approaching the 29 % limit efficiency of silicon solar cells“, *Proc of the 31<sup>st</sup> IEEE PVSEC*, Lake Buena Vista, 2005, pp. 889-894.
- [2] W. Shockley, H. J. Queisser, “Detailed Balance Limit of p-n Junction Solar Cells”, *J. of Appl. Phys.* **32**, 1961, pp. 510-519.
- [3] M. Taguchi et al., „An approach for the higher efficiency in the HIT cells“, *Proc. of the 31<sup>st</sup> IEEE PVSEC*, Lake Buena Vista, 2005, pp. 866-871.
- [4] M. Schmidt et al., “Density of gap states in extremely thin a-Si:H layers on crystalline silicon wafers”, *J. of Non-Cryst. Solids* **338-344**, 2004, pp. 211-214.
- [5] R. Stangl, M. Kriegel, M. Schmidt, “AFORS-HET, Version 2.2, a numerical computer program for simulation of heterojunction solar cells and measurements”, this conference.
- [6] Y. W. Lam, “Measurements of Commercial MIS Capacitors by the Surface-Photovoltage Method”, *Jpn. J. Appl. Phys.* **12**, 1973, pp. 916-923.
- [7] W. Henrion, et al., “Spectroscopic investigations of hydrogen termination, oxide coverage, roughness, and surface state density of silicon during native oxidation in air”, *Appl. Surf. Sci.* **202**, 2002, pp. 199-205.
- [8] H. Angermann et al., “Wet-chemical preparation and spectroscopic characterization of Si interfaces”, *Appl. Surf. Sci.* **235**, 2004, pp. 322-339.
- [9] A. Froitzheim, PhD thesis, “Hetero-Solarzellen aus amorphem und kristallinem Silizium“, Philipps-Universität Marburg, 2003.
- [10] K. Winer, L. Ley, “Surface states and the exponential valenceband tail in a-Si:H”, *Phys. Rev. B* **36**, 1987, pp. 6072-6078.
- [11] L. Korte, PhD thesis, “Die elektronische Struktur des amorph-kristallinen Silizium-Heterostruktur-Kontakts“, Philipps-Universität Marburg, 2006.
- [12] W. B. Jackson et al., “Conduction-band density of states in hydrogenated amorphous silicon determined by inverse photoemission”, *Phys. Rev. Lett.* **53**, 1984, pp. 1481-1484.
- [13] A. Laades, PhD thesis, “Preparation and Characterization of Amorphous/Crystalline Silicon Heterojunctions“, Technische Universität Berlin, 2005.
- [14] A. Laades et al., “Surface passivation of crystalline silicon wafers by hydrogenated amorphous silicon probed by time resolved surface photovoltage and photoluminescence spectroscopy”, *Proc. of the 19<sup>th</sup> EPVSEC*, Paris, 2004, pp. 1170-1173.
- [15] S. Dauwe et al., “Very low surface recombination velocities on p- and n-type wafers passivated with hydrogenated amorphous silicon films“, *Proc. of the 29<sup>th</sup> IEEE PVSEC*, New Orleans, 2002, pp. 1246-1249.
- [16] L. Korte, A. Laades, M. Schmidt, “Electronic states in a-Si:H/c-Si heterostructures” *J. Non-Cryst. Sol.*, 2006, in press.
- [17] K. v. Maydell et al., “Basic electronic properties and technology of TCO/a-Si:H(n)/c-Si(p) Heterostructure-solar-cells: A German Network Projekt”, *Proc. of the 20<sup>th</sup> EPVSEC*, Barcelona, 2005, 822-825.
- [18] K. v. Maydell, E. Conrad, M. Schmidt, „Efficient silicon heterojunction solar cells based on p- and n-type substrates processed at temperatures <220°C“, *Prog. in Photovolt.*, in press.
- [19] E. Conrad et al. „Optimization of interface properties in a-Si:H/c-Si heterojunction solar cells“, this conference.